

Implications of hyposaline stress for seaweed morphology and biomechanics

*Original*

Implications of hyposaline stress for seaweed morphology and biomechanics / Vettori, D.; Nikora, V.; Biggs, H.. - In: AQUATIC BOTANY. - ISSN 0304-3770. - 162:(2020). [10.1016/j.aquabot.2019.103188]

*Availability:*

This version is available at: 11583/2971294 since: 2022-09-14T10:09:42Z

*Publisher:*

Elsevier B.V.

*Published*

DOI:10.1016/j.aquabot.2019.103188

*Terms of use:*

This article is made available under terms and conditions as specified in the corresponding bibliographic description in the repository

*Publisher copyright*

Elsevier postprint/Author's Accepted Manuscript

© 2020. This manuscript version is made available under the CC-BY-NC-ND 4.0 license  
<http://creativecommons.org/licenses/by-nc-nd/4.0/>. The final authenticated version is available online at:  
<http://dx.doi.org/10.1016/j.aquabot.2019.103188>

(Article begins on next page)

# Implications of hyposaline stress for seaweed morphology and biomechanics

*Davide Vettori<sup>a,b\*</sup>, Vladimir Nikora<sup>a</sup>, Hamish Biggs<sup>a,c</sup>*

<sup>a</sup> *School of Engineering, University of Aberdeen, Aberdeen AB24 3UE, Scotland, UK*

<sup>b</sup> *Present address: Department of Environment, Land and Infrastructure Engineering, Politecnico di Torino, Torino 10129, Italy*

<sup>c</sup> *Present address: National Institute of Water and Atmospheric Research (NIWA), Christchurch 8011, New Zealand*

*\*Corresponding author. Email: [davide.vettori@polito.it](mailto:davide.vettori@polito.it)*

## 1. Introduction

Seaweeds are foundation species of coastal and estuarine ecosystems. They are high-yielding primary producers (Reed et al., 2008) that form important habitats for invertebrates and fish (Christie et al., 2009). In addition to the biological and ecological importance of seaweeds, they have many commercial uses, with seaweed-derived components (such as hydrocolloids) being used in cosmetics, pharmaceuticals, and food processing (Lucas and Southgate, 2012). Seaweeds are also central to Integrated Multi-Trophic Aquaculture methods (Chan et al., 2006; Chopin and Sawnhey, 2009; Lamprianidou et al., 2015) and have been successfully tested as tools for bioremediation (Fei, 2004; Wu et al., 2017). Additionally, seaweeds are an ideal source of biomass for production of third generation bio-fuels (Hughes et al., 2012; Wargacki et al., 2012).

The high utility of seaweeds and increasing global demand necessitate large scale farming (seaweed aquaculture), where biomass accrual rates should be maximised, while maintaining seaweed health (and product quality, Hughes et al., 2012). These objectives present a practical engineering challenge for the design of seaweed farms that optimally utilise light and nutrients, yet constrain the effects of hydrodynamic forcing to prevent mechanical failure (Lucas and Southgate, 2012; Buck and Langan, 2017). Seaweed growth rates are highly dependent on currents, which transport nutrient rich water into seaweed farms, and turbulence of various scales, which enhances mass exchange (Hurd, 2000; Hurd et al., 2014). For example, blade scale turbulence favours the renewal of the boundary layer, replacing depleted water with nutrient rich water (Koch, 1994; Stevens et al., 2003). Designing seaweed farms that effectively utilise natural hydrodynamics, yet are not destroyed during extreme events (storms) is an ongoing challenge. The design of aquaculture farms is usually addressed by either reduced scale physical modelling or numerical simulations (O'Donncha et al., 2013). Both of these approaches require input data on organism hydrodynamics (e.g. drag forces and drag coefficients) and mechanics (e.g. breaking stress and bending modulus). It is critical that these input data are of high quality and free of any systematic errors or biases.

Previous studies of flow-seaweed interactions and seaweed biomechanics have investigated how seaweeds have evolved to survive in habitats characterised by extreme drag forces (e.g. Koehl and Wainwright, 1977; Denny, 1988; Hurd and Stevens, 1997; Denny and Gaylord, 2002; Harder et al., 2004; Boller and Carrington, 2006; Martone et al., 2012).

Detailed investigations of seaweed reconfiguration mechanisms are commonly performed in artificial flumes (e.g. Hurd and Stevens, 1997; Boller and Carrington, 2006; Boller and Carrington, 2007; Vettori and Nikora, 2019). Due to technical limitations (e.g. preventing pump corrosion), these tests are sometimes performed in freshwater rather than saltwater/seawater (e.g. Harder et al., 2004; Buck and Buchholz, 2005; Mach, 2009; Xu et al., 2018; Vettori and Nikora, 2019). While it is practically convenient to test seaweeds in freshwater, it has not been established how hyposaline stress can affect their mechanical properties and, therefore, their hydrodynamics. Seaweeds are also temporarily exposed to hyposaline conditions (typically referred to as brackish water) in a range of natural environments, for example: seawater dilution by river water, or heavy runoff in estuaries and the nearshore zone (Kirst, 1989; Hurd et al., 2014); seawater dilution by ice-shelf melting in boreal coasts (Bold and Wynne, 1985; Karsten, 2007; Spurkland and Iken, 2011); and direct exposure to rain at low tide in the intertidal zone. For structural and economic reasons, seaweed aquaculture is likely to develop at nearshore sites such as fjords, lochs, or inlets, where seaweeds may be frequently exposed to temporary hyposaline conditions. The effects of environmental stresses such as temperature, salinity and desiccation on seaweed physiology have been recently investigated (e.g. Biskup et al., 2014; Flores-Molina et al., 2014; Wang et al., 2019). While it is accepted that salinity variations affect seaweed biochemistry and physiology (Hurd et al., 2014), we are not aware of any study focusing on how seaweed biomechanics may change. This knowledge gap must be addressed before laboratory data on flow-seaweed interactions can be used to design large scale seaweed farms (Vettori and Nikora, 2018).

This work focuses on the kelp *Saccharina latissima* (order Laminariales), a seaweed species widespread along the shores of the North Atlantic that has high commercial and ecological value. *S. latissima* is an euryhaline species (Druehl, 1967) that can live in water with salinity as low as 10‰ (Karsten, 2007; Spurkland and Iken, 2011; Mortensen, 2017). However, Nielsen et al. (2014) suggested that the growth of *S. latissima* is already reduced at salinity as low as 20‰ in the Baltic Sea. Both Karsten (2007) and Spurkland and Iken (2011) reported a strong reduction in photosynthetic activity and health status of blade tissues of *S. latissima* exposed to hyposaline stress in boreal coasts. The aim of this paper is to report the effects of short-term exposure to hyposaline stress on morphological parameters and mechanical properties of blades of *S. latissima*. Morphological parameters of the blades were characterised prior to and after exposure to freshwater. Mechanical properties of the blades

were evaluated via tensile and bending tests performed on samples after exposure to freshwater. These results are compared to the mechanical properties of blades presented in Vettori and Nikora (2017), which are used as a control (i.e. no exposure to freshwater). In particular, we test the hypotheses that seaweed blades exposed to freshwater undergo: (1) morphological modifications; and (2) changes to their mechanical properties, such as bending modulus and toughness.

## 2. Materials and methods

### 2.1 Seaweed collection and storage

Independent individuals (sporophytes) of *S. latissima* were collected on the 10<sup>th</sup> of February 2015 from long-lines deployed by Loch Fyne Oysters Limited in Loch Fyne, Scotland (56.08 N, 5.28 W). Only sporophytes free from epiphytic bryozoans and other fouling epiphytes and without obvious signs of deterioration were collected. The mean salinity and temperature in February where the seaweed samples were collected was approximately 30‰ (Gillibrand, 2002) and 7°C (<http://www.bodc.ac.uk>). Sporophytes were transported to the University of Aberdeen in barrels filled with seawater, then transferred to a 125 L aerated seawater storage tank within 8 hours of collection. The storage tank was kept outdoors in such a way that the sporophytes were exposed to natural temperature and light conditions. During the study storage water temperatures fluctuated between 3 and 8°C. Seawater in the tank was replaced every 3-4 days with seawater from the North Sea collected near Aberdeen with a mean salinity of approximately 34‰ (Janssen et al., 1999). Sporophytes were stored for up to 14 days until the tests were completed. Sporophytes that showed signs of deterioration (e.g. flaws, nicks, fissures) were discarded.

### 2.2 Experimental design

In the current study we used 23 independent sporophytes of lengths varying between 150 and 650 mm. Sporophytes were exposed to freshwater for different times ranging from 5 to 60 minutes by immersing them in a 10 L plastic container filled with freshwater at room temperature (13-15°C). Sporophytes were exposed to freshwater in separate containers, one for each sporophyte. Before exposing a sporophyte to freshwater, it was kept indoors in a container filled with seawater until water temperature reached 10-13°C. This way, we exposed sporophytes to room temperature gradually and minimised any effect of temperature shock. The morphological properties of the blades were determined prior to and after

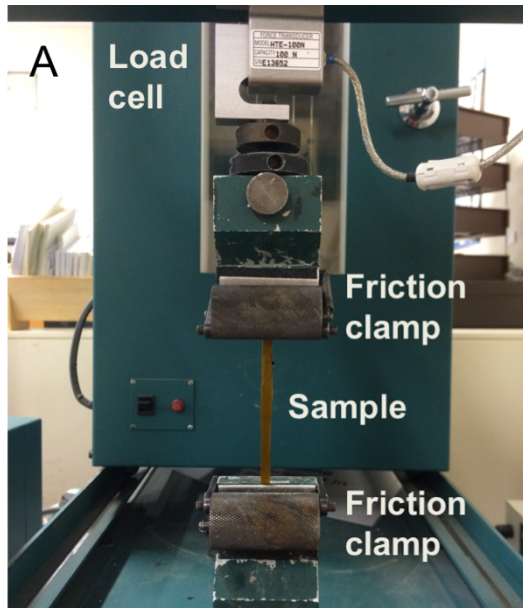
freshwater exposure. The mechanical properties of the blade material were investigated after the morphological analysis, as mechanical tests required damaging the blade by cutting samples from it.

### *2.3 Determination of morphological parameters*

This study focused on seaweed blades so the stipe was detached from each sporophyte prior to any test or measurement. For morphological assessment of a blade, a standard procedure was followed: (i) water from the blade surface was removed and then the blade was weighed using a digital scale; (ii) photos of the blade were taken with a calibrated digital camera on a light table to evaluate full-one-side blade surface area using MATLAB® (The MathWorks, Inc., Natick, Massachusetts, US); (iii) blade length, maximum width, minimum thickness, and maximum thickness were measured using rulers and callipers; and (iv) blade volume was measured by volumetric displacement in a measuring cylinder partially filled with freshwater at room temperature. Since measurements of volumetric displacement lasted a few seconds, we assumed that they did not affect results of morphological measurements or mechanical tests carried out subsequently. The morphology of 23 seaweed blades was assessed.

### *2.4 Determination of mechanical properties*

Mechanical properties of seaweed blades were determined from tension and bending tests following the procedure described in Vettori and Nikora (2017). Samples were cut from seaweed blades along the central fascia and were prepared carefully to avoid any flaws or nicks. The length to width ratio of samples was equal to or higher than 10 to avoid substantial end-wall effects (Niklas, 1992).



B

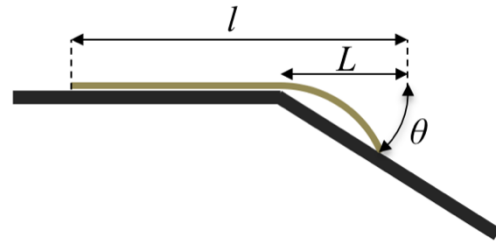


**Figure 1** Benchtop testing machine used to conduct tensile tests to sample breakage and cyclic loading-unloading tests (A); testing plate used to conduct Peirce's cantilever tests (B) with the parameters  $l$ ,  $L$ , and  $\theta$  used to calculate the bending Young's modulus.

Uniaxial tensile tests were conducted with a benchtop testing machine (Figure 1A; H10K-S UTM, Tinius Olsen, Salfords, UK) equipped with a 100 N load cell (HTE, Tinius Olsen, Salfords, UK). Two types of uniaxial tensile tests were performed: (i) tests to sample breakage; and (ii) cyclic loading-unloading tests. Prior to a test, the sample ends were secured by two friction clamps, with a sample length of 60 mm between the clamps (see also Vettori and Nikora, 2017). During the test, the upper clamp moved with a constant speed of 20 mm/min. The data on force  $F$  and displacement  $\delta$  were recorded with a dedicated software supplied by Tinius Olsen, and were later converted to nominal stress  $\sigma$  and strain  $\varepsilon$  using the formulas  $\sigma = F/A$  and  $\varepsilon = \delta/l_0$ , where  $A$  is the sample cross-sectional area, and  $l_0$  is the sample length prior to testing. The relative error of the force reading was 1.5% for force below 2 N and 0.1% for force above 2 N, calculated via independent calibration.

**Table 1** Summary of symbols and definitions of mechanical properties considered in the current study

Mechanical property	Symbol	Definition
Tensile Young's modulus	$E_t$	$E_t = \sigma/\varepsilon$ <p>where <math>\sigma</math> is nominal stress and <math>\varepsilon</math> is nominal strain (i.e. <math>E_t</math> is the slope of <math>\sigma = f(\varepsilon)</math> in the linear region at small <math>\varepsilon</math>, Figure 2A).</p>

Bending Young's modulus	$E_b$	$E_b = \frac{3 mg L^3 \cos(\theta/2)}{2 w l t^3 \tan \theta}$ <p>where <math>g</math> is gravity acceleration; <math>m</math>, <math>l</math>, <math>w</math>, and <math>t</math> are the mass, length, width and thickness of the sample; <math>\theta</math> is the inclination of the testing apparatus and <math>L</math> is the cantilever length (Figure 1B)</p>
Breaking stress	$\sigma_{br}$	Value of stress when a sample breaks (Figure 2A)
Breaking strain	$\varepsilon_{br}$	Value of strain when a sample breaks (i.e. maximum strain, Figure 2A)
Toughness	$U$	$U = \int_0^{\varepsilon_{br}} \sigma d\varepsilon$ <p>i.e., amount of energy per unit volume a sample can dissipate before breaking (Figure 2A)</p>
Elastic hysteresis	$U_{hyst}$	$U_{hyst} = \int_0^{\varepsilon_{tot}} \sigma_{load} d\varepsilon - \int_{\varepsilon_{rec}}^{\varepsilon_{tot}} \sigma_{unload} d\varepsilon$ <p>where <math>\varepsilon_{tot}</math> is the maximum strain and <math>\varepsilon_{rec}</math> is the residual strain (due to plastic deformation) after the sample has been unloaded (Figure 2B)</p>
Resilience	$R$	$R = \int_{\varepsilon_{rec}}^{\varepsilon_{tot}} \sigma_{unload} d\varepsilon / \int_0^{\varepsilon_{tot}} \sigma_{load} d\varepsilon$ <p>as illustrated in Figure 2B)</p>

144

145 Tensile tests to sample breakage were used to determine: tensile Young's modulus  $E_t$ ;  
146 breaking stress  $\sigma_{br}$  and strain  $\varepsilon_{br}$ ; and toughness  $U$ , which is the amount of energy per unit  
147 volume (J/m<sup>3</sup>) that the sample can dissipate before breaking (Table 1, Figure 2A; Vettori and  
148 Nikora, 2017).



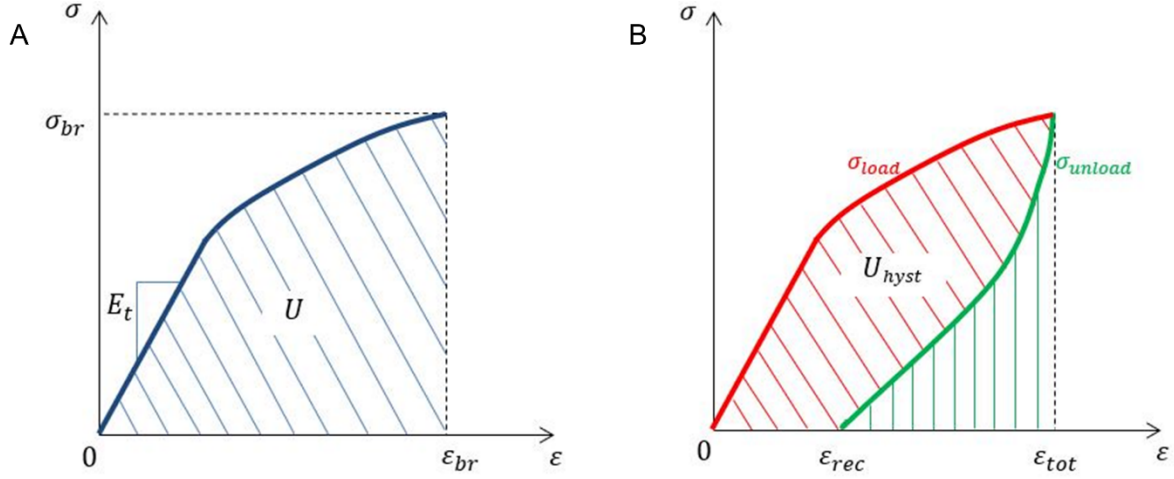


**Figure 2** Representation of stress-strain curves for: (A) tensile tests to sample breakage and (B) cyclic loading-unloading tests. In (A) the diagonal hatched area represents toughness. In (B) the diagonal hatched area represents elastic hysteresis (adapted from Vettori and Nikora, 2017).

Cyclic loading-unloading tests were performed by stretching the sample to a strain of 20% and then unloading it (with the cycle repeated three times). These tests were used to determine the elastic hysteresis and resilience. The elastic hysteresis  $U_{hyst}$  can be defined as the energy per unit volume dissipated internally during a loading-unloading cycle (Table 1, Figure 2B; Niklas, 1992). The resilience  $R$  is the ratio of the energy recovered by the sample during the unloading phase to the energy dissipated during the loading phase within a cycle (Table 1, Figure 2B; Vettori and Nikora, 2017).

Bending tests to obtain the bending modulus  $E_b$  were conducted using Peirce's cantilever test (Peirce, 1930). This test was used successfully by Henry (2014) and Vettori and Nikora (2017) to estimate the bending modulus of seaweeds. It is conducted on a plate with inclination  $\theta$ , and it requires measuring the so-called cantilever length  $L$  from which the bending modulus of a sample can be estimated (Table 1, Figure 1B; Henry, 2014).

The number of samples that were prepared from a blade depended on the size of the blade; however at least two samples for tests to sample breakage were prepared from each blade. Further, it was assumed that samples sourced along the same blade were independent of one another. It is important to note that bending tests required the use of samples substantially longer than those for other tests (Vettori and Nikora, 2017), thus the number of bending tests performed was smaller than the number of tensile tests. The numbers of samples used in each type of measurement or test are listed in Table 2 grouped by the types

of tests and five ranges of freshwater exposure times. The number of samples used in mechanical tests at exposure times lower than 20 minutes is limited because after morphological measurements were conducted, blades had to be stored in freshwater while samples were prepared and tests conducted (Table 2). In this study we also make use of biomechanics data on *S. latissima* reported in Vettori and Nikora (2017) as a control - that is, with no exposure to freshwater – comprising 25 tests to breakage, 14 cyclic tests, and 11 bending tests.

**Table 2** Numbers of samples used for morphological measurements and mechanical tests grouped by exposure times.

Freshwater exposure time (mins)	Morphological measurements	Tests to breakage	Cyclic tests	Bending tests
1-9	6	0	0	3
10-19	5	1	6	3
20-39	6	17	3	4
40-60	6	13	9	0
>60	0	23	6	4
Total	23	54	24	14

## 2.5 Statistical analysis

To investigate potential effects of hyposaline stress on blade morphology, variations in morphological parameters were standardised for each sample using  $\Delta_x = 100(x_{post} - x_{pre})/x_{pre}$ , where  $x_{post}$  is the value of a parameter after treatment, and  $x_{pre}$  is the value of the same parameter before treatment (using the Lilliefors test of normality we verified that  $\Delta_x$  for each morphological parameter was normally distributed; homogeneity of variance was confirmed via visual inspection of the residual plots). To test the hypothesis that blade morphological parameters vary as a function of time  $t$  of exposure to freshwater, each  $\Delta_x$  was analysed by applying one-way analysis of variance to linear regression. To test the hypothesis that mechanical properties of blade material vary as a function of  $t$ , we applied one-way analysis of variance to linear regression for each mechanical property introduced in the previous section. To evaluate the effect of the storage time (i.e. in the aerated storage tank) on the mechanical properties of blade material, we checked if any significant correlation between them existed. To do so, we used one-way analysis of variance to test if the slope of the linear regression between the storage time and a mechanical property differed significantly from 0. We found no significant effect of storage time on mechanical properties (ANOVA: for  $E_b$   $F_{1,26} = 1.14$ ,  $p = 0.30$ ; for  $E_t$   $F_{1,77} = 2.38$ ,  $p = 0.13$ ; for  $\sigma_{br}$   $F_{1,77} = 2.29$ ,  $p =$

0.13; for  $\varepsilon_{br}$   $F_{1,77} = 1.38$ ,  $p = 0.24$ ; for  $U$   $F_{1,77} = 0.02$ ,  $p = 0.90$ ; for  $U_{hyst}$   $F_{1,33} = 0.99$ ,  $p = 0.33$ ; for  $R$   $F_{1,33} = 0.08$ ,  $p = 0.78$ ). Data processing and statistical analysis were conducting using MATLAB with the Statistics and Machine Learning Toolbox Version 2016a (The MathWorks, Inc., Natick, Massachusetts, US). Significance for all analyses was set at  $\alpha = 0.05$ .

### 3. Results

#### 3.1 Morphology

When exposed to freshwater, the seaweed blades experienced morphological changes that became apparent within 1 hour. Over time, the blades appeared to wither/bleach and blisters filled with water developed underneath the cortex in the distal region (Figure 3B). These effects were in qualitative agreement with the findings of Karsten (2007) and Spurkland and Iken (2011) on tissue samples cut from blades of *S. latissima* from Svalbard (Norway) and Alaska (USA), respectively.

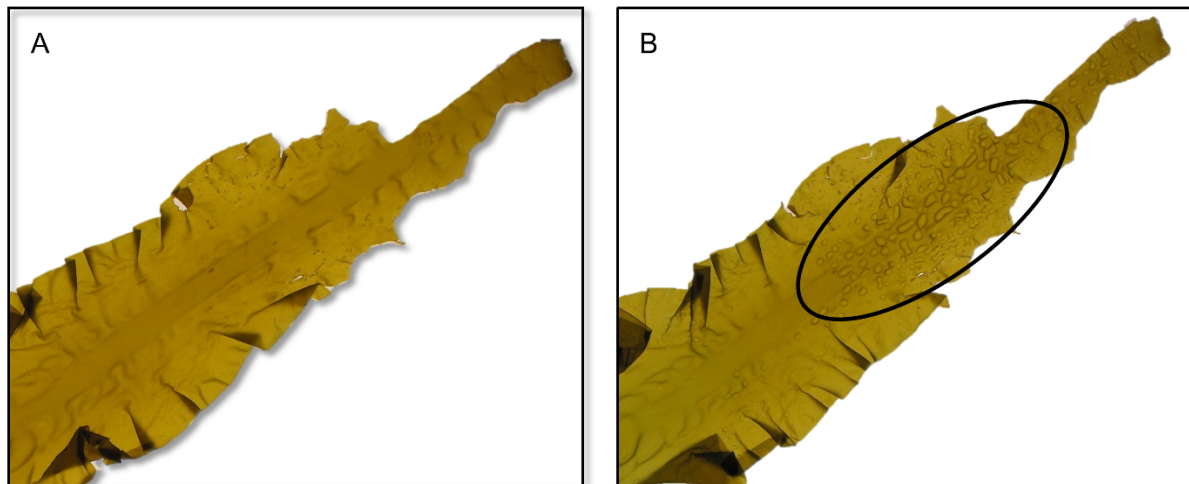


**Figure 3** Visual comparison of an upper portion of blade prior to (A) and after (B) 60 minutes exposure to freshwater. The response to hyposaline stress consists of a change in colour and the formation of water blisters beneath the cortex (area where blisters formed is highlighted with a black oval in B).

Average blade width and full-one-side surface area were significantly reduced after exposure to freshwater (Table 3), indicating that blades shrank as a response to hyposaline stress. The change in full-one-side surface area occurred at an average rate of -0.13% per minute (ANOVA:  $F_{1,22} = 21.3$ ,  $p < 0.001$ ) and the change in average width at -0.12% per

minute (ANOVA:  $F_{1,22} = 26.5$ ,  $p < 0.001$ ; Table 2). Simultaneously, average blade thickness (ANOVA:  $F_{1,22} = 11.4$ ,  $p = 0.003$ ) and weight (ANOVA:  $F_{1,22} = 6.3$ ,  $p = 0.02$ ) increased significantly, with an average rate of 0.31% and 0.14% per minute, respectively (Table 3). In the treatment with one hour exposure time, the morphological changes were significant (e.g. full-one-side surface area was reduced by 7.8% and average thickness increased by 18.8%) with implications for flow-seaweed interactions. The length of seaweed blades did not show significant patterns depending on the time of exposure to freshwater. It is worth noting that the coefficient of determination ( $R^2$ ) was quite low for linear regressions for all morphological parameters (Table 3). This illustrates the substantial scatter of the data, which is likely due to random variability between samples, or other factors which were not accounted for.

**Table 3** Variation in morphological parameters of seaweed blades as a function of time of exposure to freshwater, results of one-way ANOVA applied to linear regressions (intercept was set equal to zero). Confidence interval at  $p = 95\%$  is reported. The p-value associated with the hypothesis that the slope of the linear regression is null is reported.

	Lower C. I. Slope (%/min)	Mean Slope (%/min)	Upper C. I. Slope (%/min)	p-value	$R^2$
<b>Length</b>	-0.025	-0.007	0.012	0.478	0.050
<b>Width (avg.)</b>	-0.173	-0.124	-0.074	<0.001	0.335
<b>Thickness (avg.)</b>	0.121	0.313	0.505	0.003	0.184
<b>Surface area</b>	-0.187	-0.129	-0.071	<0.001	0.279
<b>Volume</b>	-0.045	0.171	0.388	0.125	0.057
<b>Weight</b>	0.025	0.145	0.266	0.020	0.122

### 3.2 Biomechanics

The Lilliefors test rejected the hypothesis that  $E_t$ ,  $\sigma_{br}$ ,  $U$  and  $R$  are normally distributed, however data were not transformed because we can safely assume the sample size (i.e., 79 for tensile tests, 35 for cyclic tests) is large enough to prevent bias due to sample non-normality (Underwood, 1997). Homogeneity of variance was checked via visual inspection of the residual plots and such inspection did not reveal any obvious deviation from the assumption of homoscedasticity. Blade material became more flexible (at small deformations) in both tension and bending, which was reflected by significant reductions in tensile Young's modulus  $E_t$  (ANOVA:  $F_{1,77} = 17.1$ ,  $p < 0.001$ ) and bending modulus  $E_b$  (ANOVA:  $F_{1,26} = 3.8$ ,  $p = 0.062$ ) with  $t$  (Figure 4). For one-hour exposure to freshwater this manifests as  $E_t$  decreasing from 4 MPa to 1.7 MPa, and  $E_b$  decreasing from 4 MPa to 0.8

MPa, a reduction of 57% and 80%, respectively. In Figure 4 both linear and power law regressions are shown for  $E_t$  and  $E_b$ . Linear regressions are used to test if changes in time are significant, whereas power-type approximations fit the data better (see  $R^2$  in Figure 4) and are able to account for the physical reality that moduli will not change indefinitely with a constant rate (as implied for linear regressions). The power-type regressions plotted in Figure 4 are  $E_t = 3.084t^{-0.131}$  and  $E_b = 1.907t^{-0.205}$ , respectively.

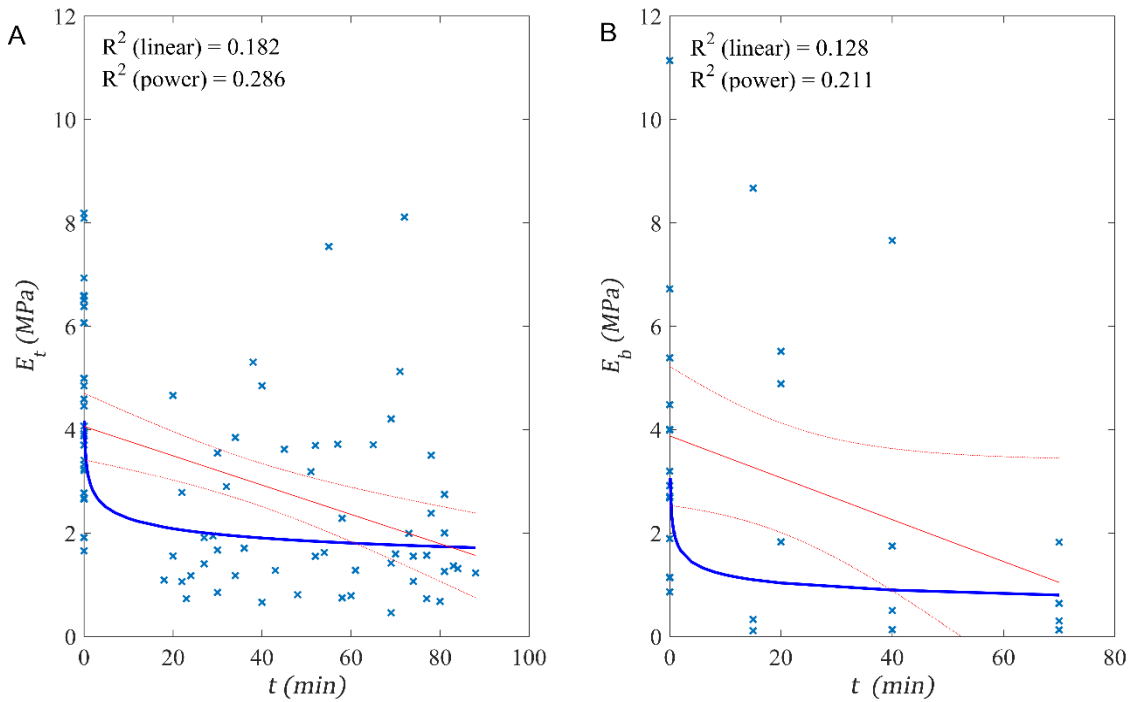


**Figure 4** Scatter plots of tensile (A) and bending (B) Young's moduli versus freshwater exposure time with linear regression and confidence interval at  $p = 95\%$  (dashed lines), and power law regression. In each plot the coefficient of determination for both linear and power law regressions is reported.

Unexpectedly, all parameters at breakage revealed a significant positive trend as a function of  $t$  (ANOVA: for  $\sigma_{br}$   $F_{1,77} = 16.1$ ,  $p < 0.001$ ; for  $\varepsilon_{br}$   $F_{1,77} = 32.8$ ,  $p < 0.001$ ; for  $U$   $F_{1,77} = 31.3$ ,  $p < 0.001$ ), meaning that after exposure to freshwater the material became more resistant to tensile stress and more energy was required to break it (Figure 5A-C). After 90 minutes of exposure to freshwater,  $\sigma_{br}$ ,  $\varepsilon_{br}$  and  $U$  showed increases of 63%, 100% and 150% respectively. Increased flexibility with exposure times also led to significant changes in properties determined from the first cycle of cyclic loading-unloading tests, with the elastic hysteresis  $U_{hyst}$  decreasing (ANOVA:  $F_{1,33} = 4.8$ ,  $p = 0.036$ ) and the resilience  $R$  increasing (ANOVA:  $F_{1,33} = 21.7$ ,  $p < 0.001$ ) (Figure 5D-E).

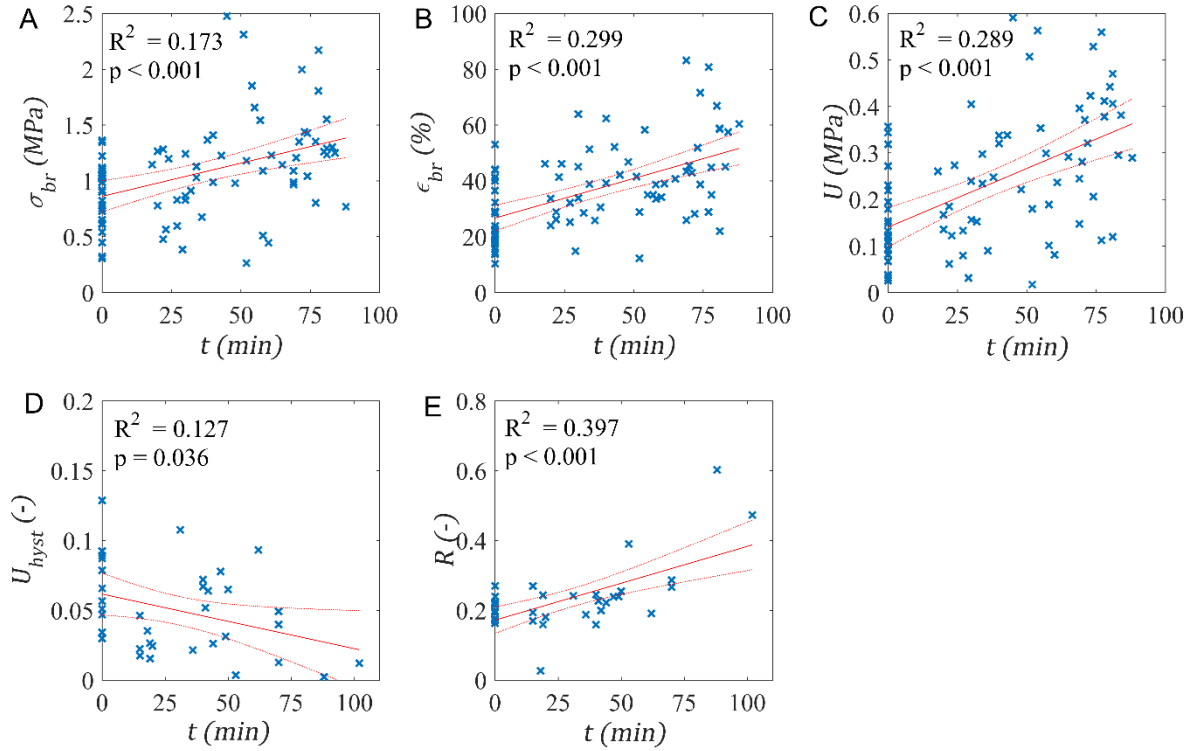


**Figure 5** Scatter plots of mechanical properties versus freshwater exposure time with linear regression and confidence interval at  $p = 95\%$  (dashed lines). In each plot the coefficient of determination and the  $p$ -value associated with the hypothesis that the slope of the linear regression is null are reported. From tests to sample breakage: (A) breaking stress, (B) breaking strain, and (C) toughness. From the first cycle of cyclic loading-unloading tests: (D) elastic hysteresis, and (E) resilience.

Even though mechanical properties are significantly affected by exposure to freshwater, it is worth noting that the coefficients of determination for linear regressions have low values ( $R^2 = 0.127$  to  $0.397$  in Figure 5). The results of one-way analysis of variance applied to linear regressions of mechanical properties versus  $t$  are reported in Table 4.

**Table 4** Variation in mechanical properties of seaweed blades as a function of freshwater exposure time, results of one-way ANOVA applied to linear regressions. The elastic hysteresis and resilience are reported for the first cycle only. The  $p$ -value associated with the hypothesis that slope of the linear regression is null is reported.

	Samples	Linear regression equation ( $t$ is time (min))	p-value	$R^2$
$E_b$ (MPa)	28	$E_b = 3.88 - 4.05 \times 10^{-2}t$	0.062	0.128
$E_t$ (MPa)	79	$E_t = 4.06 - 2.84 \times 10^{-2}t$	<0.001	0.182
$\sigma_{br}$ (MPa)	79	$\sigma_{br} = 0.861 + 5.94 \times 10^{-3}t$	<0.001	0.173
$\epsilon_{br}$ (-)	79	$\epsilon_{br} = 0.267 + 2.84 \times 10^{-3}t$	<0.001	0.299
$U$ (MJ/m <sup>3</sup> )	79	$U = 0.140 + 2.52 \times 10^{-3}t$	<0.001	0.289
$U_{hyst}$ (MJ/m <sup>3</sup> )	35	$U_{hyst} = 6.16 \times 10^{-2} - 3.91 \times 10^{-4}t$	0.036	0.127
$R$ (-)	35	$R = 0.172 + 2.11 \times 10^{-3}t$	<0.001	0.397

## 4. Discussion

### 4.1 Morphology

The main physiological process via which seaweeds adapt to salinity variations is referred to as turgor pressure regulation (Kirst, 1989). Blade morphological change is a consequence of the osmotic gradient between a blade and the medium in which it is immersed, with a blade achieving a new steady state via osmotic adjustment (Kirst, 1989; Hurd et al., 2014). In the present case, freshwater was absorbed by the blades causing blisters to develop underneath the cortex in some locations on the blades. This mechanism can damage seaweed tissue and cause cell walls to burst (e.g. Hurd et al., 2014). As a countermeasure, some cells can release metabolites to lower turgor pressure and contribute to osmotic adjustment (Niklas, 1992). We suggest this be the case for blades of *S. latissima*, which secreted a sugary liquid after being immersed in freshwater. This liquid is assumed to be mannitol, which is present in high concentrations in *S. latissima* (e.g. Adams et al., 2009), and was reported by Reed and Wright (1986) to be excreted by *Pilayella littoralis* (a brown macroalga) in response to hypoosmotic stress. Turgor pressure was not measured during this study, so it is unknown how it varied with freshwater exposure time. However, it is generally accepted that turgor pressure in seaweeds increases in response to hyposaline conditions (e.g. Hurd et al., 2014).

The morphology of seaweed blades used in the present study was significantly modified by short-term exposure to hyposaline stress. The blades absorbed freshwater, which increased the blade thickness, weight and volume. The increase in blade thickness caused corresponding reductions in blade width and blade surface area. Decreasing surface area might be a self-defending mechanism, as it allows blades to reduce the area through which exchange of fluids with the surrounding hyposaline water occurs, hence limiting the intake of hyposaline water and secretion of metabolites. Reduction of blade surface area may also have physical implications, for example to lessen viscous skin friction exerted on the blade, thus decreasing the overall drag force (Vettori and Nikora, 2019). However, it is important to note that seaweed responses to hyposaline stress reported in this study may be specific of seaweeds living in waters with high salinity (salinity at the site is around 30‰) and supplementary research conducted with samples from different environments (e.g. the Baltic Sea) would help validate our results.

## 4.2 Biomechanics

Tensile and bending Young's moduli are crucial parameters for describing the deformation of a body exposed to hydrodynamic forces. We found that both tensile and bending moduli decreased significantly with time of exposure to freshwater (Figure 4), with typical reductions of around 57% and 80% in one hour, respectively. These results are in contrast with previous findings – for example, Reed et al. (1980) reported an increase in volumetric elastic modulus of cells from a red alga in hyposaline conditions - and expectations, since we would expect seaweed blades to become stiffer as the turgor pressure increases. To explain why blade material flexibility is increased by hyposaline stress we propose the following three reasons:

- (i) Simple geometrical considerations following findings of seaweed morphological changes: samples increased their volume keeping constant length, leading to increased cross-sectional area, with a consequent reduction in the value of Young's modulus obtained from tests. These morphological considerations can account for about 20% of total reduction reported here.
- (ii) Seaweed cell walls contain cellulose (Hurd et al., 2014), which is reported to become stiffer as it gets drier (Niklas, 1992). As seaweed blades absorb freshwater (for turgor pressure regulation), cell walls are more exposed to water and thus become more flexible.
- (iii) The secretion of metabolites from parenchyma tissues (for osmotic adjustment) lowers turgor pressure and, consequently, causes a reduction in material Young's modulus (Niklas, 1992).

Cyclic tests are useful to study how seaweed material 'reacts' to periodic loads, such as those experienced due to waves. In this study we pulled samples to 20% deformation in each cycle, hence applying a loading that could occur under extreme conditions (e.g. large waves) in natural settings. A reduction in the elastic hysteresis  $U_{hyst}$  indicated that less energy is dissipated for the same deformation after exposure to freshwater. While this reduction was particularly significant for the 1<sup>st</sup> cycle, it also had a considerable effect on the 2<sup>nd</sup> and 3<sup>rd</sup> cycles. Associated with a reduction in  $U_{hyst}$  was an increase in the resilience  $R$ , which indicated that blades experienced reduced plastic deformation when exposed to freshwater, i.e. they experienced limited permanent deformations and were able to recover better from previous loadings.



The fact that  $\sigma_{br}$ ,  $\varepsilon_{br}$ , and  $U$  were positively correlated with the time of exposure to freshwater was unexpected and suggests that either: (i) seaweed tissues are strengthened as a response to hyposaline stress; or (ii) unstressed seaweeds have a survival strategy that facilitates blade rupture prior to reaching the maximum capabilities of the blade materials. The first speculation would indicate that the observed biomechanical responses to freshwater exposure are a beneficial trait that evolved in seaweeds to enable them to better withstand the environmental conditions characterising the nearshore zone. This, however, appears to be unlikely considering the short time scale of the treatment and the reduction in health status of seaweed tissues exposed to hyposaline conditions reported by Kartsen (2007) and Spurkland and Iken (2011). The second hypothesis could relate to the fact that *S. latissima* blades lose distal portions when growing older (Lee, 2008). This strategy can prevent seaweeds from experiencing extreme drag forces by reducing their surface area, particularly in winter, and could somewhat be disabled when seaweeds experience strong hyposaline stress. As the mechanical behaviour of an organism is regulated by the properties of all tissues comprising it, to shed light on the processes behind the mechanical variations reported in the present work, a study on the effects of hyposaline stress on individual tissues would be required.

It is important to note that the coefficient of determination for linear regressions was quite low for both morphological parameters and mechanical properties (Tables 3-4). It follows that the regressions presented cannot describe the variance of the data fully and cannot give accurate predictions, but only general trends. For morphological parameters this was likely caused by the high variability of seaweed blade morphology associated with the local conditions in which samples were grown (e.g. Gerard, 1987). For mechanical properties low goodness of fit was representative of the high variability in seaweed biomechanical characteristics, which was likely caused by the presence of tissues of different ages (Krumhansl et al., 2015) and blade adaptations to localised hydrodynamics. This variability was exacerbated by the use of blades of various lengths (from 150 to 650 mm) and samples being prepared from different positions along the blades (Vettori and Nikora, 2017). Further, we note that any linear regression presented here should not be used to extrapolate values of morphological parameters or mechanical properties, because the rates of change reported in this study would not apply indefinitely. Power-type approximations shown in Figure 4 for  $E_t$  and  $E_b$ , on the other hand, are more likely to represent the trends for a wider range of exposure times.

The freshwater treatment used in this study represents an extreme case for natural settings, where changes in salinity usually occur more slowly. However, in the nearshore zone, seaweeds may be temporarily exposed to very low salinity during: low tide and river floods in estuaries (e.g. Hurd et al., 2014; Mortensen, 2017); strong ice melting phenomena in boreal coasts (e.g. Spurkland and Iken, 2011); and rain events if seaweeds are exposed at low tide. While it is of limited direct ecological relevance, using an abrupt change in salinity allowed us to gain insight into changes that could not be easily detected otherwise and that we expect to also occur when seaweeds are exposed to hyposaline conditions more gradually. Based on the results presented, we can speculate that seaweeds experience lower drag forces when exposed to hyposaline stress (due to increased flexibility and morphological changes) and are less susceptible to breakage (due to increased breaking stress, breaking strain, toughness and resilience).

Findings of this study can have implications for the prediction of seaweed hydrodynamics and mechanical failure due to hydrodynamic forcing, with direct applications in the farming of seaweeds in nearshore areas and testing of seaweeds in freshwater in laboratories (e.g. Buck and Buchholz, 2005; Mach, 2009; Xu et al., 2018; Vettori and Nikora, 2019). Seaweed farming structures are designed based on the drag forces acting on the structure and the seaweeds attached to it (Lucas and Southgate, 2012; Buck and Langan, 2017). If seaweeds experience lower drag forces when exposed to hyposaline stress, that would have to be accounted for in the design phase. In hydraulic laboratories it is often convenient to test seaweeds in freshwater (e.g. Buck and Buchholz, 2005; Xu et al., 2018), but it is critical that data of drag forces acting on seaweeds are free of biases or errors that can be induced by water salinity (Vettori and Nikora, 2019). In this context, being able to assess variations in seaweed biomechanics is important for predicting the forces seaweed samples experience and the forces required to induce mechanical failure. Supplementary research with sporophytes collected from different environments would be of scientific value and help validate our results.

It is well established that exposure to hyposaline conditions affect seaweed physiology (e.g. Spurkland and Iken, 2011; Mortensen, 2017). This study provides evidence that seaweed morphological parameters and mechanical properties are also significantly affected. This has important implications for how seaweeds interact with flow and should be considered when studying seaweeds in laboratories, estuaries and the intertidal zone. Our results showed that in one hour Young's modulus in tension ( $E_t$ ) and bending modulus ( $E_b$ )

typically decreased by 57% and 80%, respectively, suggesting that seaweeds become significantly more flexible. The data also indicated that blade material becomes much more difficult to break (i.e. toughness increased by 130% in an hour). Another important factor was the reduction of blade surface area, which has implications for both physical and biological processes. Findings of this work have direct relevance for the development of seaweed farming in the nearshore zone and the study of seaweed hydrodynamics in hydraulic laboratories where saltwater cannot be employed.

## Acknowledgements

The authors are grateful to David Attwood for assistance during seaweed collection and Olivia McCabe for assistance with mechanical testing and measurement of seaweed morphology. The Northern Research Partnership, University of Aberdeen, European Community's Horizon 2020 Programme (through the grant of the Integrated Infrastructure Initiative HYDRALAB+, contract no. 654110) and Sustainable Water Allocation Programme of the National Institute of Water and Atmospheric Research of New Zealand (project CDPD1706) provided financial and methodological support to this work. This study involved data from Marine Scotland - Aberdeen Marine Laboratory, provided by the British Oceanographic Data Centre. The Editor and two anonymous reviewers provided helpful criticisms and suggestions which improved the quality of the final manuscript.

## 426 References

- 427 Adams, J. M., Gallagher, J. A. & Donnison, I. S., 2009. Fermentation study on *Saccharina*  
428 *latissima* for bioethanol production considering variable pre-treatments. *J. Appl. Phycol.*  
429 21(5):569-574.
- 430 Biskup, S., Bertocci, I., Arenas, F. & Tuya, F., 2014. Functional responses of juvenile kelps,  
431 *Laminaria ochroleuca* and *Saccorhiza polyschides*, to increasing temperatures. *Aquat. Bot.*  
432 113:117-122.
- 433 Bold, H. C., & Wynne, M. J., 1985. *Introduction to the Algae*. Prentice-Hall, Inc., Englewood  
434 Cliffs, New Jersey, 720 pp.
- 435 Boller, M. L., & Carrington, E., 2006. The hydrodynamic effects of shape and size change  
436 during reconfiguration of a flexible macroalga. *J. Exp. Biol.* 209(10):1894-1903.
- 437 Boller, M. L., & Carrington, E., 2007. Interspecific comparison of hydrodynamic  
438 performance and structural properties among intertidal macroalgae. *J. Exp. Biol.*  
439 210(11):1874-1884.
- 440 Buck, B. H., & Buchholz, C. M., 2005. Response of offshore cultivated *Laminaria saccharina*  
441 to hydrodynamic forcing in the North Sea. *Aquaculture*. 250(3):674-691.
- 442 Buck, B. H., & Langan, R., (eds) 2017. *Aquaculture Perspective of Multi-Use Sites in the*  
443 *Open Ocean: The Untapped Potential for Marine Resources in the Anthropocene*. Springer,  
444 Berlin, Germany, 404 pp.
- 445 Chan, C. X., Ho, C. L., & Phang, S. M., 2006. Trends in seaweed research. *Trends Plant Sci.*  
446 11(4):165-166.
- 447 Chopin, T., & Sawhney, M., 2009. *Seaweeds and their mariculture*. *Encycl. Ocean Sci.* 4477-  
448 4487.
- 449 Christie, H., Norderhaug, K. M., & Fredriksen, S., 2009. Macrophytes as habitat for fauna.  
450 *Mar. Ecol. Prog. Ser.* 396(1):221-233.
- 451 Denny, M., 1988. *Biology and the mechanics of wave-swept environment*. Princeton  
452 University Press, Princeton, Massachusetts, 344 pp.
- 453 Denny, M., & Gaylord, B., 2002. The mechanics of wave-swept algae. *J. Exp. Biol.*  
454 205(10):1355-1362.

455 Druehl, L. D., 1967. Distribution of two species of *Laminaria* as related to environmental  
456 factors. *J. Phycol.* 3:103–108.

457 Fei, X., 2004. Solving the coastal eutrophication problem by large scale seaweed cultivation.  
458 *Hydrobiologia.* 512(1-3):145-151.

459 Flores-Molina, M.R., Thomas, D., Lovazzano, C., Núñez, A., Zapata, J., Kumar, M., Correa,  
460 J.A. & Contreras-Porcia, L., 2014. Desiccation stress in intertidal seaweeds: Effects on  
461 morphology, antioxidant responses and photosynthetic performance. *Aquat. Bot.* 113:90-99.

462 Gerard, V.A., 1987. Hydrodynamic streamlining of *Laminaria saccharina* Lamour. in  
463 response to mechanical stress. *J. Exp. Mar. Biol. Ecol.* 107:237–244.

464 Gillibrand, P. A., 2002. Observations and model simulations of water circulation and  
465 transport in Loch Fyne, a Scottish fjord. FRS Marine Laboratory, Aberdeen.

466 Harder, D. L., Speck, O., Hurd, C. L., & Speck, T., 2004. Reconfiguration as a prerequisite  
467 for survival in highly unstable flow-dominated habitats. *J. Plant Growth Regul.* 23(2):98-107.

468 Henry, P. Y. T., 2014. Bending properties of a macroalga: adaptation of Peirce's cantilever  
469 test for in situ measurements of *Laminaria digitata* (Laminariaceae). *Am. J. Bot.*  
470 101(6):1050-1055.

471 Hughes, A. D., Kelly, M. S., Black, K. D., & Stanley, M. S., 2012. Biogas from macroalgae:  
472 is it time to revisit the idea?. *Biotechnol. Biofuels.* 5(86):1-7.

473 Hurd, C. L., 2000. Water motion, marine macroalgal physiology, and production. *J. Phycol.*,  
474 36(3):453-472.

475 Hurd, C. L., & Stevens, C. L., 1997. Flow visualization around single and multiple-bladed  
476 seaweeds with various morphologies. *J. Phycol.* 33(3):360-367.

477 Hurd, C. L., Harrison, P. J., Bischof, K., & Lobban, C. S., 2014. *Seaweed Ecology and*  
478 *Physiology*. Cambridge University Press, Cambridge, UK, 566 pp.

479 Janssen, F., Schrum, C. & Backhaus, J.O., 1999. A climatological data set of temperature and  
480 salinity for the Baltic Sea and the North Sea. *Deutsche Hydrographische Zeitschrift.* 51(Suppl  
481 9):5.

482 Karsten, U., 2007. Salinity tolerance of Arctic seaweeds from Spitsbergen. *Phycol. Res.*  
483 55(4):257-262.

484 Kirst, G. O., 1989. Salinity tolerance of eukaryotic marine algae. *Annu. Rev. Plant Physiol.*  
 485 *Plant Mol. Biol.* 40:21–53.

486 Koch, E. W., 1994. Hydrodynamics, diffusion-boundary layers and photosynthesis of the  
 487 seagrasses *Thalassia testudinum* and *Cymodocea nodosa*. *Mar. Biol.* 118(4):767-776.

488 Koehl, M. A. R., & Wainwright, S. A., 1977. Mechanical adaptations of a giant seaweed.  
 489 *Limnol. and Oceanogr.* 22(6):1067-1071.

490 Krumhansl, K. A., Demes, K. W., Carrington, E. and Harley, C. D., 2015. Divergent growth  
 491 strategies between red algae and kelps influence biomechanical properties. *Am. J. Bot.*,  
 492 102(11):1938-1944.

493 Lamprianidou, F., Telfer, T., & Ross, L. G., 2015. A model for optimization of the  
 494 productivity and bioremediation efficiency of marine integrated multitrophic aquaculture.  
 495 *Estuar. Coast. Shelf Sci.* 164:253-264.

496 Lee, R. E., 2008. *Phycology*. Cambridge University Press, Cambridge, UK, 560 pp.

497 Lucas, J. S., & Southgate, P. C., 2012. *Aquaculture: farming aquatic animals and plants*.  
 498 Wiley-Blackwell, Hoboken, New Jersey, 648 pp.

499 Mach, K. J., 2009. Mechanical and biological consequences of repetitive loading: crack  
 500 initiation and fatigue failure in the red macroalga *Mazzaella*. *J. Exp. Biol.* 212:961-976.

501 Martone, P. T., Kost, L., & Boller, M., 2012. Drag reduction in wave-swept macroalgae:  
 502 alternative strategies and new predictions. *Am. J. Bot.* 99(5):806- 815.

503 Mortensen, L. M., 2017. Diurnal carbon dioxide exchange rates of *Saccharina latissima* and  
 504 *Laminaria digitata* as affected by salinity levels in Norwegian fjords. *J. Appl. Phycol.*, 29(6):  
 505 3067-3075.

506 Nielsen, M. M., Krause-Jensen, D., Olesen, B., Thinggaard, R., Christensen, P. B. & Bruhn,  
 507 A., 2014. Growth dynamics of *Saccharina latissima* (Laminariales, Phaeophyceae) in Aarhus  
 508 Bay, Denmark, and along the species' distribution range. *Mar.Biol.*, 161(9):2011-2022.

509 Niklas, K. J., 1992. *Plant biomechanics: an engineering approach to plant form and function*.  
 510 University of Chicago Press, Chicago, Illinois, 607 pp.

511 O'Donncha, F., Hartnett, M., & Nash, S., 2013. Physical and numerical investigation of the  
 512 hydrodynamic implications of aquaculture farms. *Aquacult. Eng.* 52:14-26.

513 Peirce, F. T., 1930. The “handle” of cloth as a measurable quantity. *J. Text. Inst. Trans.*  
514 21:T377-T416.

515 Reed, R. H., Collins, J. C. & Russell, G., 1980. The effects of salinity upon cellular volume  
516 of the marine red alga *Porphyra purpurea* (Roth) C. Ag. *J. Exp. Bot.* 31(6):1521-1537.

517 Reed, D. C., Rassweiler, A., & Arkema, K. K., 2008. Biomass rather than growth rate  
518 determines variation in net primary production by giant kelp. *Ecology.* 89(9):2493-2505.

519 Reed, R. H., & Wright, P. J., 1986. Release of mannitol from *Pilayella littoralis* (Phaeophyta:  
520 Ectocarpales) in response to hypoosmotic stress. *Mar. Ecol. Prog. Ser.* 29:205-208.

521 Spurkland, T., & Iken, K., 2011. Salinity and irradiance effects on growth and maximum  
522 photosynthetic quantum yield in subarctic *Saccharina latissima* (Laminariales,  
523 Laminariaceae). *Bot. Mar.* 54:355-365.

524 Stevens, C. L., Hurd, C. L., & Isachsen, P. E., 2003. Modelling of diffusion boundary-layers  
525 in subtidal macroalgal canopies: The response to waves and currents. *Aquat. Sci.* 65(1):81-91.

526 Underwood, A. J., 1997. *Experiments in ecology: their logical design and interpretation*  
527 *using analysis of variance*. Cambridge, UK, University Cambridge Press, 504 pp.

528 Vettori D., & Nikora V., 2017. Morphological and mechanical properties of blades of  
529 *Saccharina latissima*. *Estuar. Coast. Shelf. S.* 196:1-9.

530 Vettori D., & Nikora V., 2018. Flow–seaweed interactions: a laboratory study using blade  
531 models. *Environ. Fluid Mech.* 18(3):611-636.

532 Vettori, D., & Nikora V., 2019. Flow-seaweed interactions of *Saccharina latissima* at a blade  
533 scale: turbulence, drag force, and blade dynamics. *Aquat. Sci.* 81(4):61.

534 Wang, W.J., Li, X.L., Zhu, J.Y., Liang, Z.R., Liu, F.L., Sun, X.T., Wang, F.J. & Shen, Z.G.,  
535 2019. Antioxidant response to salinity stress in freshwater and marine *Bangia* (Bangiales,  
536 Rhodophyta). *Aquat. Bot.* 154:35-41.

537 Wargacki, A. J., Leonard, E., Win, M. N., Regitsky, D. D., Santos, C. N. S., Kim, P. B.,  
538 Cooper, S. R., Raisner, R. M., Herman, A., Sivitz, A. B., Lakshmanaswamy, A., Kashiyama,  
539 Y., Baker, D., & Yoshikuni, Y., 2012. An engineered microbial platform for direct biofuel  
540 production from brown macroalgae. *Science.* 335(6066):308-313.

541 Wu, H., Kim, J.K., Huo, Y., Zhang, J. & He, P., 2017. Nutrient removal ability of seaweeds  
542 on *Pyropia yezoensis* aquaculture rafts in China’s radial sandbanks. *Aquat. Bot.* 137:72-79.

543 Xu, M., Sasa, S., Otaki, T., Hu, F.X., Tokai, T. & Komatsu, T., 2018. Changes in drag and  
544 drag coefficient on small *Sargassum horneri* (Turner) C. Agardh individuals. *Aquat. Bot.*  
545 144:61-64.